ELSEVIER

Since January 2020 Elsevier has created a COVID-19 resource centre with free information in English and Mandarin on the novel coronavirus COVID-19. The COVID-19 resource centre is hosted on Elsevier Connect, the company's public news and information website.

RBD decorated PLA nanoparticle admixture with aluminum hydroxide elicit robust and long lasting immune response against SARS-CoV-2

Jairam Meena [a,c,*], Priyank Singhvi [a], Sudeepa Srichandan [a], Jyotsna Dandotiya [a], Juhi Verma [a], Mamta Singh [a], Rahul Ahuja [a], Neha Panwar [a], Tabiya Qayoom Wani [a], Ritika Khatri [b], Gazala Siddiqui [b], Anuradha Gupta [a], Sweety Samal [b], Amulya Kumar Panda [a,*,1]

[a] *Product Development Cell, National Institute of Immunology, Aruna Asaf Ali Marg, New Delhi 110067, India*
[b] *Infection and Immunology Laboratory, Translational Health Science & Technology Institute, Gurgaon-Faridabad, India*
[c] *Department of Pharmaceutical Engineering and Technology, Indian Institute of Technology (Banaras Hindu University), Varanasi, Uttar Pradesh 221005, India*

ABSTRACT

Nanoparticles-based multivalent antigen display has the capability of mimicking natural virus infection characteristics, making it useful for eliciting potent long-lasting immune response. Several vaccines are developed against global pandemic caused by severe acute respiratory syndrome coronavirus 2 (SARS-CoV-2). However these subunit vaccines use mammalian expression system, hence mass production with rapid pace is a bigger challenge. In contrast *E. coli* based subunit vaccine production circumvents these limitations. The objective of the present investigation was to develop nanoparticle vaccine with multivalent display of receptor binding domain (RBD) of SARS-CoV-2 expressed in *E. coli*. Results showed that RBD entrapped PLA (Poly lactic acid) nanoparticle in combination with aluminum hydroxide elicited 9-fold higher immune responses as compared to RBD adsorbed aluminum hydroxide, a common adjuvant used for human immunization. It was interesting to note that RBD entrapped PLA nanoparticle with aluminum hydroxide not only generated robust and long-lasting antibody response but also provided Th1 and Th2 balanced immune response. Moreover, challenge with 1 μg of RBD alone was able to generate secondary antibody response, suggesting that immunization with RBD-PLA nanoparticles has the ability to elicit memory antibody against RBD. Plaque assay revealed that the antibody generated using the polymeric formulation was able to neutralize SARS-CoV-2. The RBD entrapped PLA nanoparticles blended with aluminum hydroxide thus has potential to develop asa subunit vaccine against COVID-19.

1. Introduction

COVID-19 that is caused by one of the Coronaviridae family members, severe acute respiratory syndrome coronavirus 2 (SARS-CoV-2), has emerged as a major threat to public health worldwide [1]. As of March 22, more than 680 million people have been diagnosed with COVID-19 cases in 221 countries and more than 6 million people have died due to infection of SARS-CoV-2, according to Worldometer, Dadax Limited, USA. There are four structural proteins present in the SARS-CoV-2 viz. spike (S), envelope, membrane and nucleocapsid proteins [2]. The spike protein, particularly receptor binding domain (RBD), plays major role in the virus attachment, fusion, and its entry into the host cells with the help of angiotensin converting enzyme 2 (ACE2) present on the host cells [3]. Considering the binding of RBD with host

ACE2 receptor, RBD has been touted as one of ideal targets for vaccine development [4].

Viruses are naturally occurring nano-scale organisms which inspire nanomaterials for immunoengineering and vaccine development. Incorporation of structural features of viruses into nanoparticles using nanotechnology and nanochemistry enables efficient delivery of antigen with enhanced humoral and cellular immune response [5]. Nanotechnology has enormously contributed in RNA, DNA or protein subunit-based COVID-19 vaccine development [6–10]. Subunit vaccine candidate such as RBD constitute minimal structural component that can prime protective immune responses in the host. Poly lactic acid (PLA) or poly lactic co-glycolic acid (PLGA) are Food and Drug Administration (FDA) approved polymer for human applications. Hence, RBD-PLA nanoparticles as targeted delivery system of vaccine to antigen

presenting cells are known to generate a sustained immune response, making them preventive and therapeutic tool for wide range of diseases.

Development of a safe and effective vaccine against SARS-CoV-2 which could be manufactured at faster rate will be helpful for global immunization. An ideal COVID-19 vaccine should possess the attributes of long-lasting immune response and easy deployment to billions of people while exhibiting zero to minor side-effects. With the emergence of different variants of SARS-CoV-2 worldwide, it is of utmost importance to develop a range of COVID-19 vaccines with different mechanism of action. As of September 2021, there are 315 vaccine candidates under consideration while 121 in clinical trials (Update on September 21, 2021, retrieved from https://www.who.int/publications/m/item/draft-landscape-of-covid-19-candidate-vaccines). Till the date, most of the approved vaccines are vector-based, mRNA-based and inactivated viruses vaccines while DNA and protein subunit based vaccines are under late-stage clinical trials.

Protein subunit-based vaccines offer a range of advantages over nucleic acid based vaccines. They can be easily lyophilized and stored, thereby eliminating the need of cold-chain for global distribution of vaccine. Moreover, compelling evidences have suggested that protein subunit-based vaccines directed against SARS-CoV2 deliver potent and long-term antibody responses in animal models [6,11]. Therefore, almost 36% of vaccine candidates under investigation till the date are based on protein subunit, further substantiating its advantages over other types of vaccines.

Several protein subunit-based vaccines under 3rd and 4th clinical trial have exploited RBD as a vaccine candidate while using viral or mammalian expression systems. Viral and mammalian expression systems are ideal for the heterologous production of RBD with structure-function integrity. However, the high processing cost, time consumption and intensive care at each step involved in the production limit its scalability at industrial scale. Moreover, it has been reported that the RBD protein lacking glycosylation in its structure is immunogenic and elicits neutralizing antibodies [12]. Such practical limitations with viral and mammalian expression systems encourage exploiting better microbial cell factories for the high-throughput production of RBD.

In spite of its wide usage as a host for expression of variety of proteins, most of the COVID-19 vaccine candidates use yeast, baculovirus or mammalian expression systems, lacking either or combination of attributes viz. cost-effectiveness, deployability, long-term immune response. The objective of the present investigation was to explore the immunogenicity of RBD protein expressed in *E. coli* which could not only give a sustained immune response but also provide a cheaper, stable and deployable alternative to existing vaccine candidates. In the present report, RBD was expressed as bacterial inclusion bodies, refolded and used for immunization study. Immunogenicity of RBD was further improved by using different adjuvants including PLA based nanoparticles. Two dosages of RBD entrapped in PLA nanoparticles along with aluminum hydroxide elicited long-lasting neutralizing antibody response in BALB/c mice. Particle based delivery of vaccine formulation also elicited memory antibody response when challenged with soluble antigen. The results are of indication that *E. coli* based antigen entrapped in PLA nanoparticles along with aluminum hydroxide has potential to develop as a effective vaccine against SARS-CoV2.

2. Materials and methods

2.1. Chemicals and reagents

Culture media components such as tryptone extract and Bacto yeast extract were purchased from Difco Laboratories, India. Glucose, deoxycholic acid (DOC), sodium chloride (NaCl) and glycine were purchased from Titan Bioech Limited, India. Sodium dihydrogen phosphate was purchased from Qualigens Fine Chemicals, India. Phenylmethylsulfonyl fluoride (PMSF), isopropyl β-D-1- thiogalactopyranoside (IPTG), Acrylamide, bis-acrylamide and Tris-HCl buffer were from Amresco, USA.

Sodium dodecyl sulphate (SDS), ammonium persulfate (APS), dithiothreitol (DTT), concentrated HCl, skimmed Milk, disodium hydrogenphosphate, dihydrogen potassium phosphate, Tween 20, urea, polyvinyl alcohol (PVA, 30–70 kDa), O-phenylenediamine dihydrochloride (OPD), hydrogen peroxide (H_2O_2), carbon coated copper grids (TEM-FCF200CU) were from Sigma-Aldrich, USA. Tetramethylethylenediamine (TEMED), ethylenediaminetetraacetic acid (EDTA), chemiluminescent reagent and bromophenol blue were from BIO-RAD, USA. Coomassie brilliant blue R-250 and ampicillin were from USB Corporation, USA. Glacial acetic acid, methanol and potassium chloride were from MerckMillipore, Canada while dichloromethane, acetonitrile, H_2SO_4 were purchased from Merck, India. Ethanol and glycerol were of analytical grade and were from Spectrochem, India. DEAE- Sepharose Fast Flow media were purchased from GE Healthcare, UK. Micro bicinchoninic acid (BCA) and BCA assay kit, SDS–PAGE prestained molecular weight marker and Dulbecco's Modified Eagle Medium (DMEM) was from Thermo Scientific, USA. GFP-taggedanti-rabbit RBD antibodies was purchased from GeneTex, USA. Poly lactic acid (PLA, 45 kDa) was purchased fromPurac Holland. Phosphate Buffer Saline (PBS) was purchased from Himedia, India. Uranyl acetate was purchased from Sisco research laboratories, India. Aluminum hydroxide 2% (w/v) was purchased from Brenntag Biosector Denmark. HRP conjugated goat-antimouseIgG (H + L)(A90-116P) was purchased from eBiosciences, USA. Antimouse HRP conjugated IgG1 (SC-32322) andIgG2a (SC-271847) were purchased from Santa Cruz Biotech, USA. All other chemicals were of analytical grade. Limulus Amebocyte Lysate (LAL) kit (Catalog no-50-647U) was purchased from Lonza USA.

2.2. Expression and purification of RBD from bacterial inclusion bodies

Glycerol stock of *E. coli* cells carrying the RBD gene was inoculated in 10 mL of modified LB media {10 g Bacto-tryptone, 5 g Bacto-yeast extract, 10 g sodium chloride (NaCl), and 5 g D-glucose per Liter of MilliQ water} along with working concentration of 100 μg/mL ampicillin and incubated overnight in an orbital shaker (Kühner shaker, Switzerland) set at 200 rpm and 37 °C. 10 mL of primary culture was added to 1 L of modified LB media having working concentration of 100 μg/mL ampicillin in shaker flasks. The flasks were transferred to an orbital shaker set at 200 rpm and 37 °C and cells were induced with 1 mM working concentration of IPTG when OD_{600nm} measured in UV–Vis spectrophotometer (Amersham Biosciences, United Kingdom) arrived at 0.6 AU. Cells were allowed to grow for another 4 h in orbital shaker for expression of protein and bacterial pellet was obtained after centrifuging at 4000g for 15 min at 4 °C (Sorvall RC6+, USA). The status of RBD expression was confirmed by SDS-PAGE analysis on vertical mini-gel SDS-PAGE apparatus (Bio-Rad Laboratories, USA).

Bacterial cell pellet was resuspended from 1 L culture in 40 mL of lysis buffer (50 mM Tris-HCl, 5 mM EDTA and 1 mM PMSF, pH 8.5). The suspension was homogenized at 5,000 rpm using a homogenizer (POLYTRON® PT 3100 D Kinematica AG, Switzerland) for 1 min on ice. Further, cell suspension was sonicated for 10 cycles of 1 min each (short pulses of 1 s followed by a gap of 1 s) with 1 min gap between the cycles at 50% amplitude of sonicator (Q 700 sonicator, Qsonica, USA). The cell suspension was centrifuged at 20,000g for 30 min at 4 °C (Eppendorf 5810 R, Germany). The resulting pellet was washed by re-suspending it in 50 mL of Milli-Q water and the suspension was centrifuged at 20,000g for 30 min at 4 °C. Supernatant was discarded and the final pellet (purified IBs) was re-suspended in 2 mL Milli-Q water. The cell free extract and pellet were analysed on SDS-PAGE.

2 mL IBs was re-suspended and mixed well in 18 mL of mild solubilization formulation (2 M urea, 1 mM DTT, Milli-Q water, pH 12.5). The mixture was allowed to incubate at room temperature for at least 1 h and was vortexed 3–6 times during incubation. The solubilized protein sample was centrifuged at 20,000g for 30 min at 4 °C. Supernatant was collected and 200 μl of 12 M fuming concentrated HCl was added in 20 mL of solubilized protein to bring the pH from 12.5 to 3. The solubilized

protein sample was again centrifuged at 20,000g for 30 min at 4 °C and supernatant was collected to proceed for refolding. 80 mL of chilled refolding buffer {20 mM phosphate buffer (NaH$_2$PO$_4$ salt), Milli-Q water, pH 4.5} waskept in an ice bath under stirring conditions set at 200 rpm.20 mL solubilized protein (pH ~ 3) was diluted to the refolding buffer in dropwise fashion by using a peristaltic pump (Pharmacia LKB Pump P1, Sweden) operating at 0.5 mL/min. After incubation of the refolded protein sample at 4 °C for 6 h, the sample was centrifuged at 20,000g for 30 min at 4 °C.

100 mL of refolded protein was concentrated to 8 mL using concentrator (Pall® Centrifugal Devices, Pall Corporation, Puerto Rico) with membrane of 3 kDa molecular weight cut off.5 mL of DEAE-Sepharose column(HiTrap® DEAE Fast Flow5 mL column, GE Healthcare, UK) was connected with fast protein liquid chromatography (ÄKTA pure, GE Healthcare, UK). The column was washed with 10 column volume of Milli-Q water and then equilibrated with 10 column volume of equilibration buffer {20 mM phosphate buffer (NaH$_2$PO$_4$ salt), Milli-Q water at pH 4.5}. 8 mL of concentrated refolded protein was loaded onto equilibrated DEAE Sepharose column and flow through was collected in a beaker. Further, DEAE Sepharose was passed through elution buffer {20 mM phosphate buffer (NaH$_2$PO$_4$ salt), 500 mM NaCl, Milli-Q water, pH 4.5} and the fractions were collected and pooled. The flow through and elutes of DEAE-anion exchange chromatography were concentrated using the same concentrator. The concentration of the IBs, solubilized protein, refolded protein, concentrated flow through and elutes was measured by BCA method and analysed on SDS-PAGE.

2.3. Characterization of refolded RBD

Purified RBD protein was resolved on 10% SDS-PAGEand was transferred from the gel to the nitro cellulose membrane using transfer buffer {25 mM Tris-HCl, 192 mM glycine, 0.1% (w/v) SDS, 10% (v/v) methanol and Milli-Q water} at 40 mA for 16 h. The membrane was then washed once for 5 min with 0.1% PBST (137 mM NaCl, 2.7 mM KCl, 10 mM Na$_2$HPO$_4$, 1.8 mM KH$_2$PO$_4$, Milli-Q water, pH 7.4). The membrane was incubated in blocking buffer {3%(w/v) skimmed milk in PBST buffer} for 2 h. The membrane was further washed three times for 5 min each with 0.1% PBST followed by incubation with GFP-tagged RBD primary antibody (1:5000) for overnight at 4 °C. Later on, the membrane was again washed five times for 5 min each with 0.1% PBST. The membrane was incubated with horse radish peroxidase (HRP) conjugated secondary antibody (1:10,000) for 1 h at room temperature. The membrane was washed three times for 5 min with 0.1% PBST buffer. Signals were detected by chemiluminescence reagent (1:1 ratio of peroxide substrate and luminal reagent) after exposing the membrane to ChemiDoc imaging system (Bio-Rad Laboratories, USA).

The secondary structure of purified RBD was analyzed using far-UV circular dichroism (CD) spectroscopy (Jasco-700 spectropolarimeter, USA) at 20 °C. Spectra were recorded from195 to 250 nm for 200 µg/ml solution of purified RBD protein taken in a 1 mm path length cuvette. The CD spectrum was scanned three times and the average spectrum was plotted eventually.

2.4. 2.4Antigen dose optimization and immunization schedule

All the animal immunization studies were performed after approval of institutional animal ethics committee (IAEC no. 397/20) of National Institute of Immunology, New Delhi. 6–8 week old female BALB/c mice were randomly divided into different groups of six mice for experiments. Mice were immunized intramuscularly and blood was collected using intra-orbital puncture. Immunization schedule was optimized using different time intervals (0th, 14th and 28th day) with 5 µg purified RBD in comparison to phosphate buffer saline. Single and double dosage studies were performed and compared to each other. For single immunization study, mice were immunized with 5 µg RBD on 0th day and blood were collected on 14th day. Antibody estimation was performed

using ELISA and the results were analyzed using GraphPad Prism 6. For double immunization study, mice were immunized with 5 µg RBD on 0th day and again immunized on 14th day. Blood were collected on 16th day and antibody response was determined and analyzed. Similarly, mice were immunized with 5 µg RBD on 0th day and again immunized on 28th day. Blood were collected on 30th day and antibody response were determined and analyzed. Sera were diluted 200 times in phosphate buffer saline and ELISA was performed for all the experiments except end point titer estimation. As the expression of RBD in bacterial system often poises challenges of endotoxin contamination, the purified RBD was subjected to determination of any lipopolysaccharide present in the immunization dose as per the manufacturer's instructions of LAL kit.

Antigenic dosages were optimized with varying amount of RBD in the presence and absence of aluminum hydroxide. Different amount of RBD (5, 10 and 20 µg) were injected intramuscularly in mice in the presence of 10 µg of aluminum hydroxide. In another group, only 5 µg of RBD was used as a reference control. Blood was collected on 16th day and antibody response were determined using ELISA and analyzed on GraphPad Prism 6.

2.5. Formulation of RBD entrapped PLA nanoparticles

Poly lactic acid (PLA) nanoparticles were prepared using double emulsion solvent evaporation method [13]. 25 mg/mL of PLA polymer was dissolved in 4 mL of dichloromethane (DCM) solvent to use as an organic phase. An aqueous phase was prepared containing 7.5 mg/mL of purified RBD, 0.5% (w/v) polyvinyl alcohol (PVA) with phosphate buffer saline (PBS). For external aqueous phase, 2% (w/v) polyvinyl alcohol was dissolved in 12 mL of Milli-Q water. Primary emulsion was prepared using RBD containing internal aqueous phase and PLA containing organic phase with the help of sonication (Bandelin sonoplus, Germany; 2 min, 30% amplitude and 40% duty cycle). This primary emulsion was further sonicated into external aqueous phase using the same sonicator for (3 min, 30% amplitude and 40% duty cycle). Double emulsion was kept on constant stirring for 12 h at room temperature to evaporate the organic solvent, DCM. The nanoparticles were centrifuged at 31,200g for 20 min at 4 °C. Pellet was re-suspended in 5 mLMilli-Q water to remove the surfactant, PVA. The washing step was repeated one more time for complete removal of any residual PVA in the nanoparticles. Finally, the nanoparticles were re-suspended in 5 mLMilli-Q water and lyophilized for further use.

2.6. Characterization of RBD entrapped PLA nanoparticles

RBD-PLA nanoparticles formulated using double emulsion solvent evaporation method were characterized for particle size, zeta potential, polydispersity index (PDI), antigen load, entrapment efficiency and surface morphology. Nanoparticles were weighed and suitably diluted in Milli-Q water to avoid the multi scattering phenomenon. Nanoparticles were further analyzed for their size, zeta potential and PDI using particle size analyzer (Malvern zetasizer NanoZS, UK). Next, antigen load, amount of RBD present per mg of polymer nanoparticles, was determined using micro BCA assay [14]. For this, 10 mg of nanoparticles were dissolved in 1 mL of acetonitrile and centrifuged at 15,500g for 15 min. The polymer washing cycle was repeated for three times to completely remove the PLA polymer. Pellet was dissolved in 1% (w/v) sodium dodecyl sulphate and amount of protein was quantified using micro BCA assay. Entrapment efficiency of RBD entrapped per mg of polymer particles was determined using the following equation:

$$\frac{\text{Practical load of RBD per mg of nanoparticles}}{\text{Theoretical load of RBD per mg of nanoparticles}} \times 100$$

Surface morphology of nanoparticles was analyzed using transmission electron microscopy (TEM) (Technai G2, Phillips Holland). Antigen entrapped nanoparticles were diluted in Milli-Q water and mounted over carbon coated copper grid followed by 1% (w/v) uranyl

acetate staining. Samples were air dried and analyzed using TEM.

2.7. Adjuvant optimization for immunization

Different adjuvants such as aluminum hydroxide, aluminum phosphate, PLA nanoparticles or a combination of RBD-PLA nanoparticles with aluminum hydroxide was used for the adjuvant dose optimization. SixBLAB/c female mice were immunized with different adjuvants on 0th day and blood were collected on 14th day. ELISA was performed for the antibody estimation while saline was taken as a negative control in all the experiments. One group of female mice was immunized with 5 μg of RBD alone whereas another group was immunized with 5 μg of RBD adsorbed on 10 μg of aluminum hydroxide. In second set of experiment, 5 μg of RBD alone and 5 μg of RBD adsorbed on 10 μg of aluminum phosphate were used in immunization studies. In third set of experiment, 5 μg of RBD alone and equal amount of RBD entrapped in 746 μg of RBD-PLA nanoparticles were used in immunization studies. In the final set of experiment, 5 μg of RBD alone, equal amount of RBD entrapped in 746 μg of PLA nanoparticles and 5 μg of RBD entrapped in 746 μg of PLA nanoparticles blended with 10 μg of aluminum hydroxide.

2.8. RBD specific immune response in BALB/c mice

Four groups of six female BALB/c mice were immunized intramuscularly with saline, 5 μg RBD, 5 μg RBD adsorbed with aluminum hydroxide, equal amount of RBD entrapped PLA nanoparticles blended with aluminum hydroxide. Booster dose was given with the aforementioned formulations on 14th day. Blood were collected on 16th, 28th, 42nd, 62nd and 90th day as depicted in Fig. 5A. 1 μg of RBD alone as a memory dose was given on 91st day and blood was collected on 97th, 104th and 120th day as depicted in Fig. 5A. ELISA was performed for the estimation of antibody response.

2.9. Antibody estimation in serum of immunized BALB/c mice

1 μg of recombinant RBD was coated in high binding ELISA plates of 96 wells (RIA NUNC, ThermoFisher Scientific, USA). Plates were incubated at 4 °C for 12 h followed by blocking with 5% skimmed milk powder for 1 h at 37 °C. For total IgG estimation, goat-antimouse IgG (1:10,000 dilution in PBS) was used. Similarly, for IgG1 (1:1000 dilution in PBS) and IgG2a (1:1000 dilution in PBS) was used. Plates were washed gently with washing buffer {0.1% (v/v) Tween 20, 100 mM PBS, pH7.4} and 100 μl of sera diluted in PBS (1:200) was added to each well. The plate was incubated for 2 h at 37 °C followed by washing thrice using washing buffer. 100 μl of HRP conjugated anti-mouse secondary antibody was added in each well (1:10,000 dilution in PBS) and further incubated at 37 °C for 1 h. After incubation, plates were again washed thrice using washing buffer. 100 μl of o-phenylene diamine dihydrochloride (OPD) substrate was added in each well and was allowed for color development. Reaction was stopped using 25 μl of 2 N H_2SO_4 and plates were read at 490 nm using ELISA reader (BioTek spectrophotometer, Vermont USA).

2.10. SARS CoV-2 neutralization assay

Virus plaque-based neutralization assay was performed in the Infectious Disease Research Facility (biosafety level 3 facility) Translation Health Science and Technology Institute, New Delhi, India. Sera of six immunized BALB/c mice were collected on 28th day. Sera were pooled and 40-fold diluted with PBS. 100 μl of diluted sera was incubated with 100 μl of 20 plaque forming unit (PFU) of SARS CoV-2 isolate USAWA 1/2020. The diluted sera and virus were incubated for 1 h at 37 °C.

Confluent Vero E6 cells were then infected with sera-virus mixture in 24-well tissue culture plates followed by 1 h incubation at 37 °C. The cells were washed one time with DMEM and incubated with 2% carboxymethylcellulose containing DMEM medium for 48 h at 37 °C.

Following incubation, cells were fixed for 4 h at room temperature with 6% (v/v) formalin for virus inactivation after PBS washing. The fixed cells were stained with 1% (v/v) crystal violet and counted with naked eyes after air drying. Results were analyzed as compared to saline in the presence of hyper immune sera as positive control.

3. Results and discussion

3.1. Purification and characterization of refolded RBD from bacterial inclusion bodies

The heterologous expression of RBD gene was induced using IPTG and its expression was confirmed by SDS-PAGE at ∼26 kDa band as depicted in Fig. 1A and mentioned in Table S1. The proteins were isolated by breaking open the bacterial cells using sonication. Cell free extract and insoluble fraction after centrifugation of sheared bacterial cells were analysed on SDS-PAGE as shown in Fig. 1B. The presence of RBD protein in insoluble fraction signified its heterologous expression as bacterial inclusion bodies. pH based mild denaturing method was employed to solubilize RBD IBs in order to improve the overall yield [15]. Since RBD protein contains 9 cysteine residues as mentioned in Table S1, 1 mM DTT was also added in the formulation for disrupting the disulphide bonds. The soluble RBD protein recovered after centrifugation was loaded onto SDS-PAGE and the protein concentration was estimated using BCA method. As evident from Fig. 1C and Table 1, 76.82% protein of inclusion bodies was recovered. As mentioned in Table S1, the isoelectric point (pI) of RBD protein is 8.9, the protein tends to precipitate when the pH of the medium is between 5 and 10which may be due to lack of glycosylation machinery in *E. coli*. Therefore, a sudden change in pH from 12.5 to 3 was introduced by addition of concentrated HCl. This time, 98.78% protein was recovered from the solubilized protein at pH 12.5 step (Fig. 1C and Table 1). Solubilized protein was refolded in chilled refolding buffer {20 mM phosphate buffer (NaH_2PO_4 salt), Milli-Q water, pH 4.5} in order to minimize the intermolecular interactions of protein intermediates. The refolded protein was centrifuged to remove insoluble aggregates and was concentrated. The concentrated refolded protein was then loaded onto DEAE-anion exchange chromatography to remove the contaminants. From Fig. 1D, it was observed that there was a peak in the flow through while there was no peak observed for elutes of DEAE-anion exchange chromatography. Flow through and elutes were concentrated and analysed on SDS-PAGE. Observations from Fig. 1C and Table 1 revealed that RBD protein was present in flow through with step yield of 82.74%. The reason why RBD protein did not bind to DEAE column is attributed to the fact that the pH of the medium was 4.5 while pI of the protein was 8.9. Therefore, the protein possessed the net positive charge, making it unable to bind with DEAE-Sepharose. Finally, the refolded and purified RBD was recovered from bacterial inclusion bodies with overall yield of 53.91%.

The purified RBD protein was characterized by western blotting and circular dichroism. The presence of RBD protein among the mixture of proteins was confirmed using western blotting as shown in Fig. 1E. In addition, the purified RBD protein was found to possess secondary structure as mentioned in Fig. 1F and Table S2.

3.2. Antigen dose optimization and immunization schedule

As RBD is a promising candidate for vaccine development against COVID-19, its immunogenicity was tested by the single dose of 5 μg RBD as shown in Fig. 2A. It was observed that IgG antibody response did not change significantly as compared to saline (Fig. 2B), which suggested that the single dose of RBD (Fig. 2A & 2B) is not sufficient for evoking the immune response. This may be due to weak immunogenicity possessed by the recombinant antigens [16–17]. Therefore, two dosages schedule consisting of RBD on 0th and 14thday were tested as shown in Fig. 2C. From Fig. 2D with two doses, it was observed that there was a
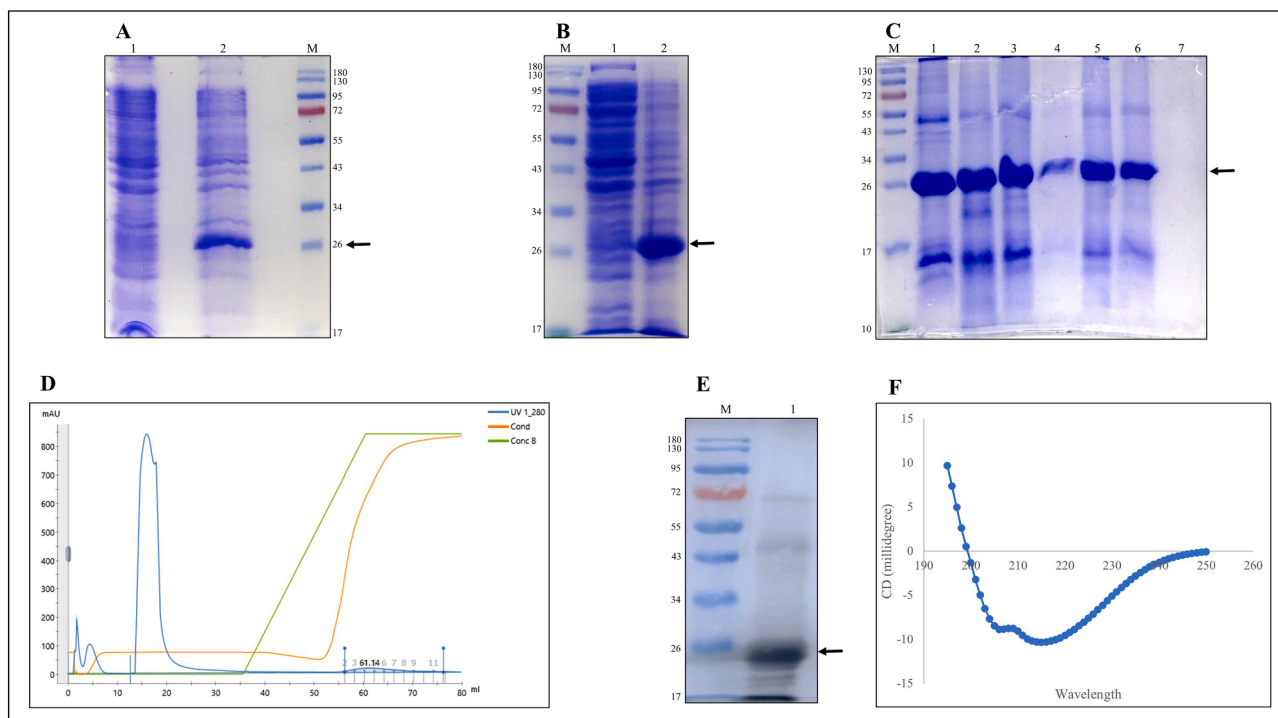
Fig. 1. Expression, purification and characterization of refolded receptor binding domain (RBD). Arrow () indicates the protein of interest. Lane M represents molecular weight marker (180, 130, 95, 72, 55, 43, 34, 26, 17 and 10 kDa). **A.** 12% SDS-PAGE analysis of RBD expression: lane 1, uninduced cell lysate; lane 2, induced cell lysate; lane M, molecular weight marker. **B.** 12% SDS-PAGE analysis of isolated inclusion bodies of RBD: lane 1, supernatant of cell lysate; lane 2, isolated RBD IBs (MW 26.3 kDa); lane M, molecular weight marker. **C.** 15% SDS-PAGE analysis of recovery of RBD from bacterial inclusion bodies: Lane M, molecular weight marker; lane 1, RBD IBs; lane 2, solubilized RBD in aqueous solution of 2 M urea, pH 12.5; lane 3, solubilized RBD in aqueous solution of 2 M urea, pH 3; lane 4, refolded RBD in 20 mM phosphate buffer, pH 4.5; lane 5, concentrated RBD protein in 20 mM phosphate buffer, pH 4.5; lane 6, flow through of DEAE ion exchange chromatography and lane 7, Elutes after DEAE ion exchange chromatography. **D.** DEAE anion exchange chromatogram for purification of refolded RBD. **E.** Identification of RBD using western blot. **F.** Secondary structure determination of RBD using far-UV circular dichroism.

Table 1
Heterologous production of RBD from bacterial inclusion bodies using pH based mild denaturing method.

Steps	Total protein (mg)	Step yield (%)	Overall yield (%)
Inclusion bodies	62.10	100	100
Solubilization at pH 12.5	47.71	76.82	76.82
Solubilization at pH 3	47.13	98.78	75.89
Refolding at pH 4.5	40.46	85.84	65.15
DEAE ion exchange chromatography	33.48	82.74	53.91

significant improvement in IgG antibody response after two doses. This signified that a booster dose is essential to evoke the antibody response against RBD. We further tested the duration of two doses for better immune response. Therefore, mice were immunized with RBD at 0th day and 28th day as shown in Fig. 2E. It was observed from Fig. 2F that two dosages with time interval of 28 days also generated significant IgG antibody response as compared to saline. On comparison to the IgG immune response generated on 14th and 28th day, it was observed from Fig. S1 that there was no significant difference in immune response between the given time intervals. Hence, two dosages schedule on 0th and 14th day was selected to get the desired protection as early as possible.

It was of interest to investigate whether the increased dosage of RBD along with an adjuvant like aluminum hydroxide could further increase the immune response without causing any notable toxicity as compared to 5 μg of RBD alone. Therefore, mice were immunized with different dosages of RBD along with aluminum hydroxide as shown in Fig. 2G. It was observed from Fig. 2H that there was no significant improvement in

the IgG response with respect to increasing dosages of RBD along with aluminum hydroxide. It was also noticed that the adsorption of RBD on aluminum hydroxide did not significantly improve the immune response as compared to RBD alone. However, aluminum hydroxide is reported to release the antigens gradually, thereby evoking the immune response on the long-term basis [18]. Therefore, further immunization studies with time intervals of two weeks were performed using 5 μg of RBD adsorbed on aluminum hydroxide. To rule out the possibility of nonspecific antibody response due to the LPS contamination, LAL test was assay performed. The results showed that the LPS present per immunization dose were 0.1 endotoxin unit which was 10-fold lower than the recommend endotoxin dose for preclinical studies [19]. This suggests that the generated immune response was not induced due to LPS contamination in the immunized antigen.

3.3. Characterization of RBD entrapped PLA nanoparticles

Compelling evidences suggests that PLA based nanoparticle favors the efficient internalization by antigen presenting cells thus elicit antigen specific immune responses [20–21]. Therefore, RBD was entrapped in RBD-PLA nanoparticles and characterization studies were carried out. Fig. 3A showed that nanoparticles are in the size of 329.9 nm. Previous reports suggest that the particles of such size are efficiently phagocytosed by antigen presenting cells and present the particles in secondary follicle organs for initiation of immune response [13]. Further, the zeta potential of nanoparticles was measured to be −14.3 mV (Fig. 3B) which suggests good colloidal stability of nanoparticles. In order to investigate the polydispersity of nanoparticles, PDI was measured to be 0.169 (Fig. 3A and 3C) suggesting that RBD entrapped nanoparticles are of homogeneous size. Transmission electron microscopy (TEM) image of
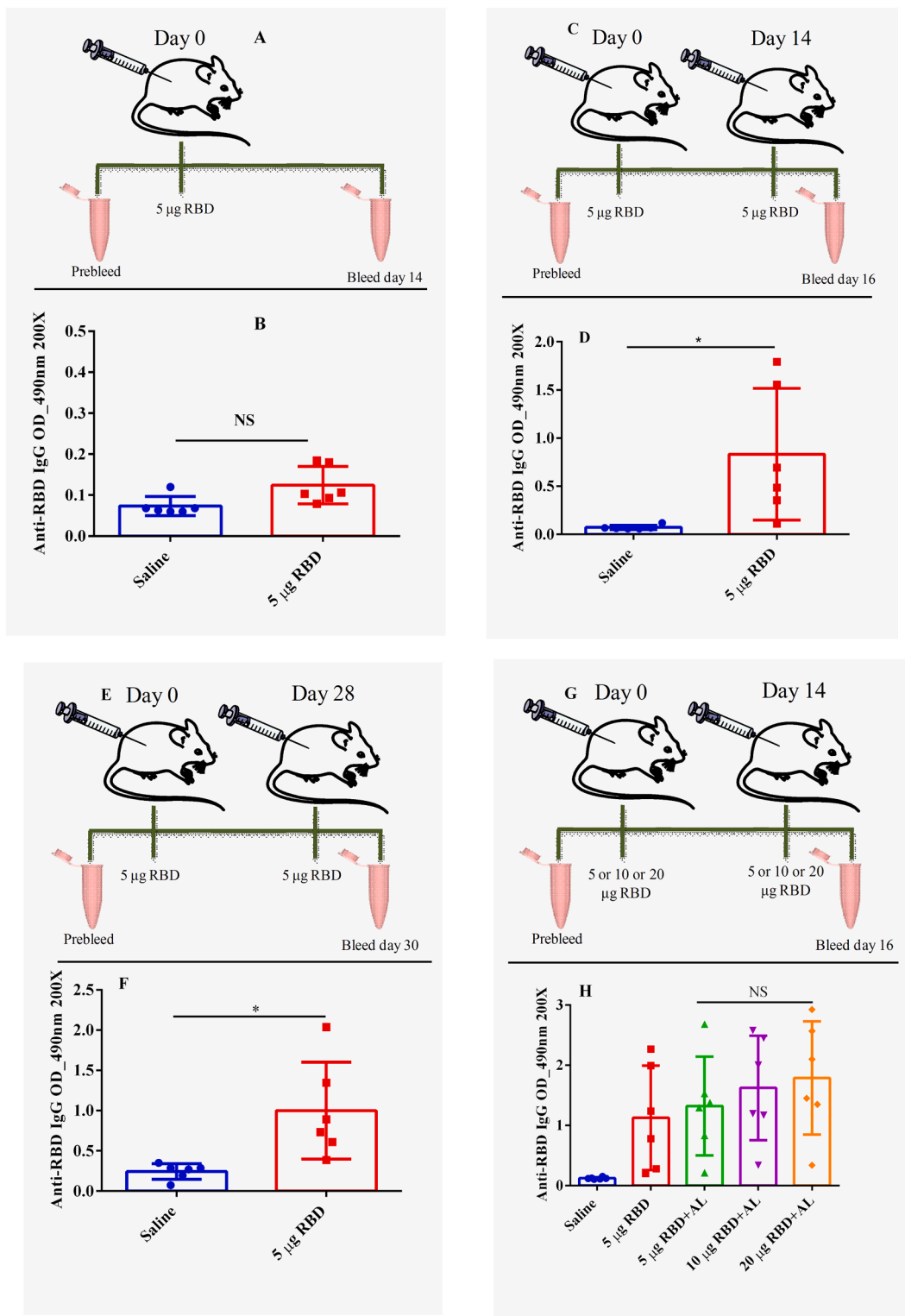
Fig. 2. RBD dosing schedule and dose optimization in BALB/c mice. A. Schematic representation of intramuscular immunization of single dose of 5 μg RBD. **B.** IgG antibody response generated with single dose of RBD. **C.** Schematic representation of intramuscular immunization of two doses of 5 μg RBD at 0th and 14th day. **D.** IgG antibody response generated with two doses of RBD at 0th and 14th day. **E.** Schematic representation of intramuscular immunization of two doses of 5 μg RBD at 0th and 28th day. **F.** IgG antibody response generated with two doses of RBD at 0th and 28th day. **G.** Schematic representation of intramuscular immunization of different doses of RBD at 0th and 14th day. **H.** IgG antibody response generated with different doses of RBD at 0th and 14th day. Statistical significant difference were calculated using unpaired student *t* test (p < 0.005).
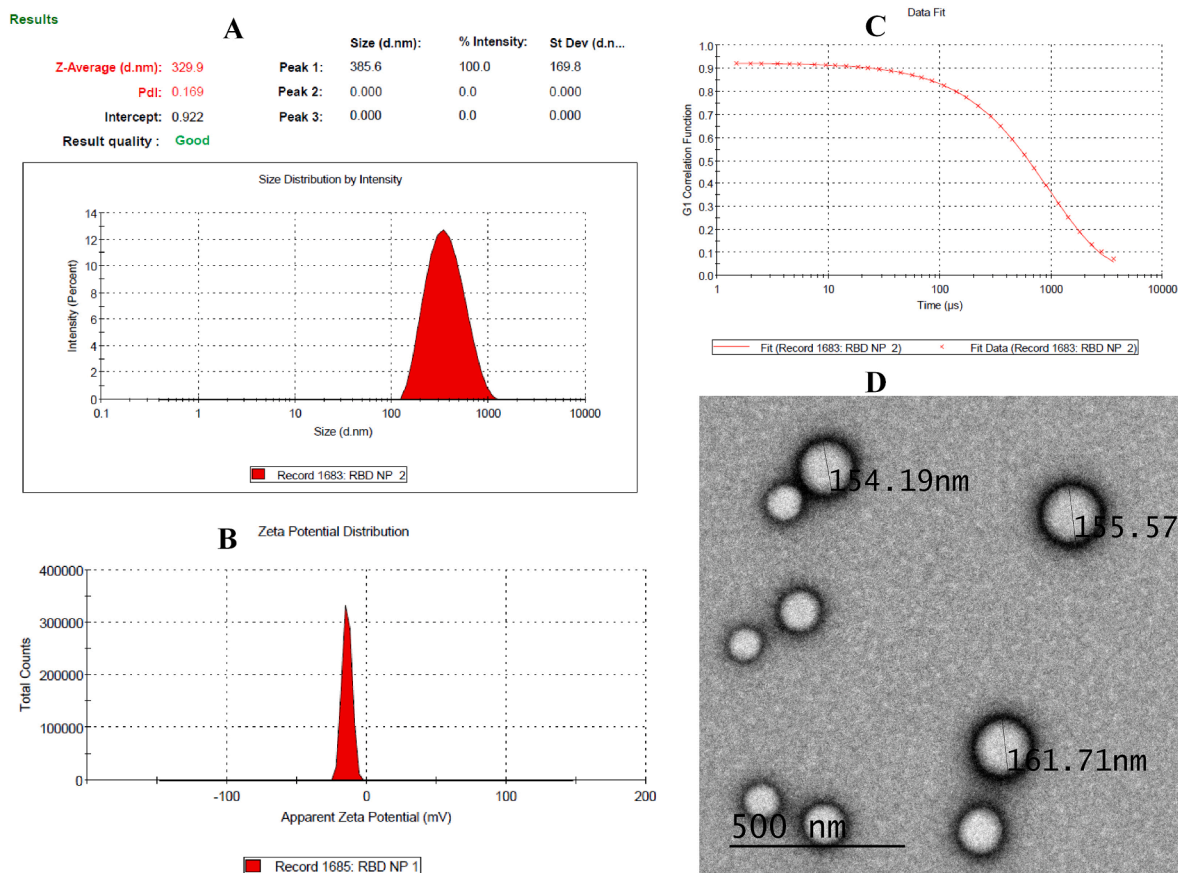
Fig. 3. Characteristics of RBD entrapped PLA nanoparticles. A. PLA nanoparticles size (diameter in nanometer). **B.** Zeta potential of PLA nanoparticles. **C.** Particle size distribution curve fit. **D.** Transmission electron microscopy (TEM) image of PLA nanoparticles.

nanoparticles has demonstrated that particles are spherical in shape and in the accordance to the size measured using Zetasizer (Fig. 3D). Finally, antigen load was determined to be 6.7 μg RBD per mg of RBD-PLA nanoparticles whereas antigen entrapment efficiency was 40%. Thus, it was established that RBD entrapped nanoparticles are potential adjuvant candidate for evoking the immune responses.

3.4. Impact of adjuvant on RBD specific immune responses

Adjuvants have been indispensable component of vaccine formulation. Aluminum hydroxide is most commonly used adjuvants in human vaccines. However, it is not compatible with all the antigens and is not be able to evoke the immunogenicity against all the antigens [22]. Therefore, it is imperative to select an adjuvant or a combination of adjuvants based on the physicochemical properties of the antigen-adjuvant complex for eliciting maximum immunogenicity. It was observed from Fig. 4A that there was no significant difference in IgG immune response against RBD adsorbed on aluminum hydroxide as compared to RBD alone on 16th day. As the isoelectric point (pI) of RBD is 8.9 (Table S1), the protein at physiological pH would be positively charged. In contrast, aluminum phosphate is reported to be negatively charged at physiological pH. Therefore, aluminum phosphate was analyzed as a potential adjuvant candidate. From Fig. 4B, it was observed that there was a significant decrease in IgG immune response as compared to RBD alone which suggested that aluminum phosphate is not compatible with RBD. Previous reports establish PLA nanoparticles as potential delivery system and adjuvant for improving the immune responses [20]. Therefore, the IgG immune response for RBD entrapped PLA nanoparticles in comparison to RBD alone was analyzed. It was observed from Fig. 4C that there was no significant improvement in

immune response as compared to RBD alone. This could be attributed to lesser antigen availability due to slow RBD release in case of RBD-PLA nanoparticles [23]. As observed from Fig. 4A and Fig. 4C, the immune response was improved, albeit not significantly, in the case of aluminum hydroxide and PLA based nanoparticles. Moreover, aluminum hydroxide is reported to evoke Th2 based immune response while PLA based nanoparticles have the potential to elicit both Th1 and Th2 immune response [13]. Therefore, aluminum hydroxide blended RBD-PLA nanoparticles were analyzed in comparison to RBD alone and RBD entrapped PLA nanoparticles. Fig. 4D revealed that the aluminum hydroxide blended RBD-PLA nanoparticles were able to improve the immune response significantly as compared to RBD alone. Hence, the aluminum hydroxide blended RBD-PLA nanoparticles were selected as final formulation for further immunization studies.

3.5. Antibody sustainability and memory recall response

An effective vaccine should have a robust and long-term immune response along with a rapid memory recall response upon re-infection of the same pathogen. These parameters were tested *in vivo* with BALB/C mice immunization studies as shown in Fig. 5A. From Fig. 5B, it was observed that aluminum hydroxide blended RBD-PLA nanoparticles generated higher immune response than RBD alone and RBD adsorbed on aluminum hydroxide. Particularly, IgG antibody response generated by aluminum hydroxide blended RBD-PLA nanoparticles was significantly higher than RBD alone on 28th day. This was interesting because there was no significant difference in antibody response between RBD alone and RBD entrapped nanoparticles on 14th day (Fig. 4C). Higher antibody response of aluminum hydroxide blended RBD-PLA nanoparticles on 28th day is attributed to the fact that RBD-PLA nanoparticles
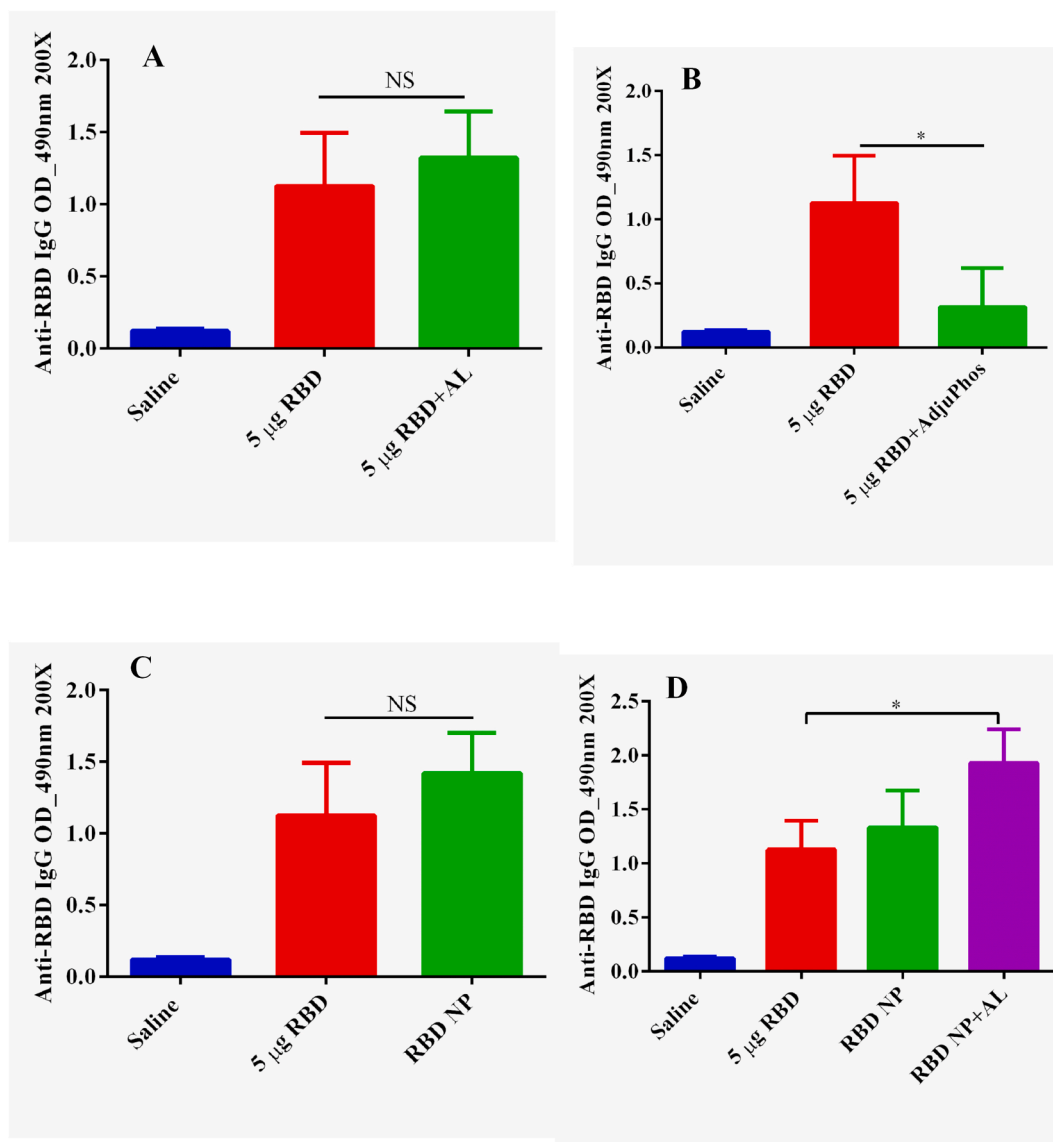
Fig. 4. Adjuvant optimization in BALB/c mice. A. Effect of aluminum hydroxide on IgG antibody response. **B.** Effect of aluminum phosphate on IgG antibody responses. **C.** Effect of PLA nanoparticles on IgG antibody response. **D.** Effect of aluminum hydroxide blended PLA nanoparticle on IgG antibody response generated against RBD. Statistical significant difference were calculated using unpaired student *t* test (p < 0.005).

would be releasing the antigen, RBD, gradually over the period of time. Thus, RBD-PLA nanoparticles and aluminum hydroxide is an ideal combination for the generation of RBD specific robust immune response. It was also observed from Fig. 5B that the antibody concentration in sera for different formulations decreased with respect to time. The IgG response generated by RBD alone reached to the saline level in 63 days. In contrast, the immune response generated by RBD adsorbed on aluminum hydroxide and aluminum hydroxide blended RBD-PLA nanoparticles was 5.27 and 7.47-fold higher than saline level even after 90 days respectively. This suggested that optimal antibody titer was maintained in case of aluminum hydroxide blended PLA nanoparticles.

The long-lasting vaccine mediated immune protections is driven by antigen specific memory B cells and memory T cells responses. Memory B cells rapidly differentiate into antibody secreting plasma cells upon re-infection with the same pathogen [24]. These plasma cells exponentially secrete the pathogen neutralizing high affinity antibodies which bind with the pathogen and clear it off from the host. Memory recall responses are highly sensitive and hence can induce robust antigen specific immune responses even with low dosage of antigen. In order to

investigate the memory recall response, mice were immunized with 1 μg of RBD on 91st day and sera were collected as shown in Fig. 5A. A rapid rise in antibody response was observed for different formulations as depicted in Fig. 5B. Moreover, the antibody response of aluminum hydroxide blended RBD-PLA nanoparticles was significantly higher than that of RBD alone and RBD adsorbed on aluminum hydroxide. However, it was observed that, despite the low doses of soluble RBD alone, all groups showed memory recall response. The memory antibody response was also sustained and did not reduce rapidly as observed on 120th day as shown in Fig. 5B. These findings suggested that hydroxide blended RBD-PLA nanoparticles evoke a robust and long-term immune response along with a rapid memory recall response.

3.6. Endpoint titer estimation

Optical density estimated in ELISA reaches to the level of saturation if the concentration of antibodies is very high. This makes it difficult to differentiate the concentration of antibodies generated against different formulations. Therefore, antibodies are serially diluted to the concentration where optical density in ELISA could be estimated in a detectable
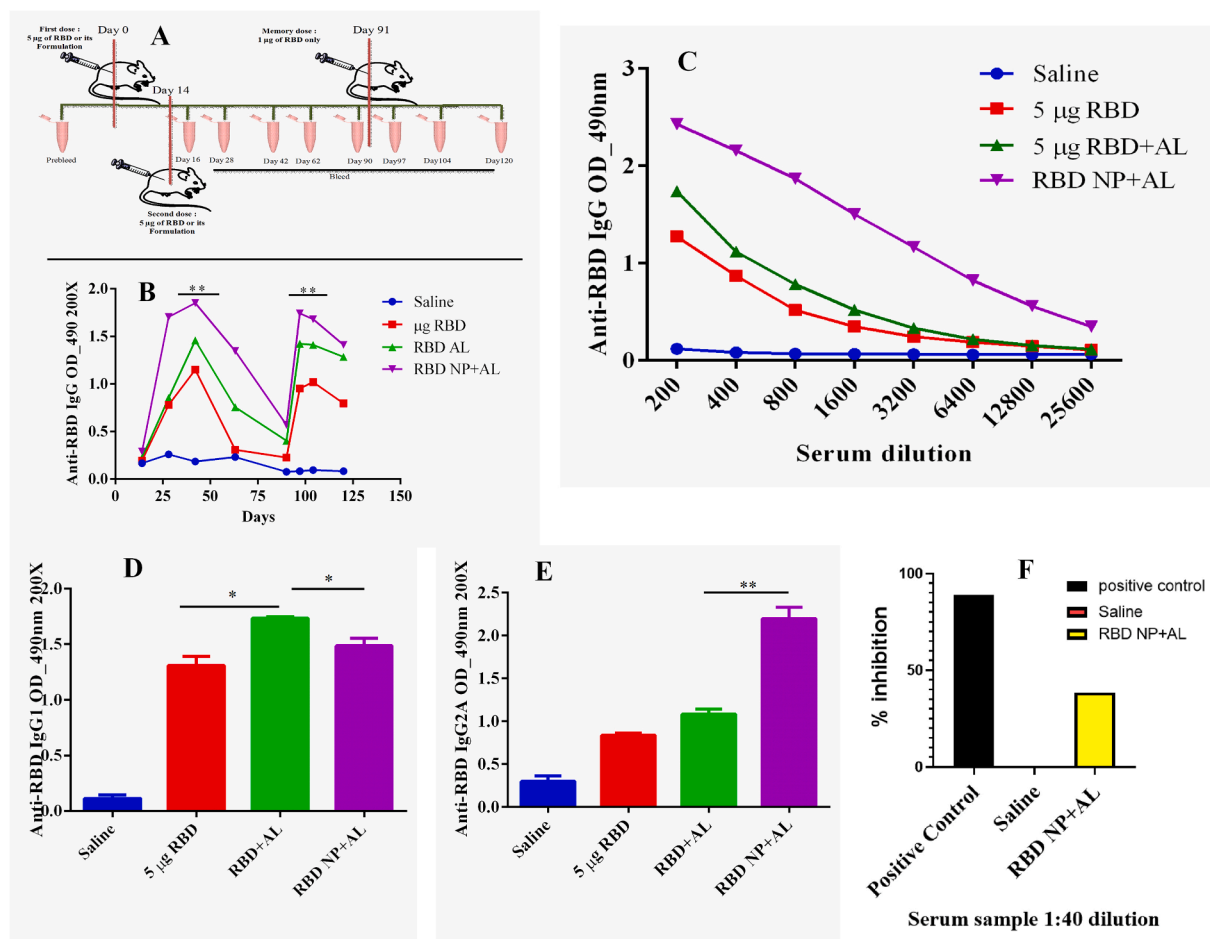
Fig. 5. **RBD specific primary and memory antibody response generated in BALB/c mice with aluminum hydroxide blended PLA nanoparticles and its virus neutralization effect. A.** Schematic representation of priming dose, booster dose and memory dose immunization. **B.** Sustainability of IgG antibody titer with time and memory antibody recall response. Statistical significant difference were calculated using one way ANOVA ($p < 0.0001$). **C.** Endpoint titer estimation for comparative fold change in antibody response. **D.** Th2 specific IgG1 immune response generated by aluminum hydroxide and aluminum hydroxide blended PLA nanoparticles. **E.** Th1 specific IgG2a immune response generated by aluminum hydroxide and aluminum hydroxide blended PLA nanoparticles. Statistical significant difference were calculated using unpaired student *t* test ($p < 0.005$). **F.** SARS CoV-2 neutralization potential of aluminum hydroxide blended PLA nanoparticles immunized sera (1:40 dilution) collected on 28th day as compared to hyper immune sera (positive control) and saline (negative control).

range. Upon 25,600-fold dilution, there was no discernible difference in the concentration of antibodies generated by RBD alone and RBD adsorbed aluminum hydroxide as compared to saline level (Fig. 5C). Interestingly, the concentration of antibodies generated by aluminum hydroxide blended RBD-PLA nanoparticles was 2.8fold higher than that of antibodies generated by RBD alone and RBD adsorbed aluminum hydroxide upon 25,600-fold dilution. The concentration of antibodies generated by aluminum hydroxide blended RBD-PLA nanoparticles reached to the saline level upon extrapolating the sera dilution to 102,400-fold. These results suggest that RBD-PLA nanoparticles blended with aluminum hydroxide significantly improve the immune response as compared to rest of the formulations.

3.7. Effect of admixture of PLA nanoparticles and aluminum hydroxide on Th1 vs Th2 response

In order to provide an efficient protection against viral infection, it is essential that a vaccine should evoke Th1 and Th2 type balanced immune response which is measured by IgG2a and IgG1 respectively [25–28]. Such response could be induced using different adjuvants in the vaccine formulation. For instance, adjuvants such as CpG oligodeoxy nucleotides, aluminum hydroxide and PLA based nanoparticles can induce Th1, Th2 and a balanced Th1-Th2 immune response respectively [29–30]. Therefore, it was of interest to investigate whether RBD

adsorbed on alum and aluminum hydroxide blended RBD-PLA nanoparticles could evoke different immune responses. From Fig. 5D, it was observed that there was a significant increase in IgG1 immune response of RBD adsorbed on aluminum hydroxide in comparison to RBD alone. This suggested that aluminum hydroxide adjuvant favors Th2 immune response. The total IgG response of aluminum hydroxide blended RBD-PLA nanoparticles as observed in Fig. 5B was significantly higher than RBD adsorbed on aluminum hydroxide. Surprisingly, a significant reduction in the IgG1 immune response of aluminum hydroxide blended RBD-PLA nanoparticles was observed as compared to RBD adsorbed on aluminum hydroxide. The decrease of IgG1 and increase of IgG2a with RBD entrapped PLA nanoparticles blended with aluminum hydroxide (Fig. 5D&5E) suggest thatTh2 immune responses (IgG1) was shifted to Th1 (IgG2a) immune response when RBD immunized as PLA nanoformulation. This signified that inclusion of RBD-PLA nanoparticles with hydroxide incites both Th1 and Th2 balanced immune response.

3.8. SARS CoV-2 neutralization assay

Having confirmed the long-term memory response and balanced Th1 and Th2 immune response, investigating the neutralization efficiency of antibodies generated against aluminum hydroxide blended RBD-PLA nanoparticles was of utmost importance for the overall success of the formulation as a potential vaccine candidate. From Fig. 5F, it was

observed that aluminum hydroxide blended RBD-PLA nanoparticles immunized sera at 1:40 dilution showed ~35% virus neutralization as compared to hyper immune sera whereas saline did not show any neutralization. This suggests that the antibodies generated against aluminum hydroxide blended RBD-PLA nanoparticles were functionally effective and possess neutralization capacity against SARS-CoV-2.

4. Conclusions

This current study investigated the potential of *E. coli* expressed RBD based polymeric nano-formulation toelicit a sustained immune response as an alternative to existing covid vaccine candidates. It was observed that RBD entrapped PLA nanoparticle blended with aluminum hydroxide was able to generate enhanced and long-term immune response *in vivo*. In addition, the formulation evokes a balanced Th1 and Th2 immune response. Concomitantly, the antibodies raised against RBD antigen were able to neutralize SARS-CoV-2. Interestingly, mimicking the natural infection condition, challenge with low dosage of only RBD elicited memory antibody response in experimental animal. Even though Th1 immune response was analyzed using IgG2a, a qualitative and quantitative evaluation of SARS-CoV-2 specific CD8 + T cells response would provide an in-depth understanding of Th1 mediated protection. Overall, the RBD entrapped PLA nanoparticle blended with aluminum hydroxide could be used as a potential protein-subunit based nanoparticle vaccine against COVID-19.

Ethics approval

All the animal studies were performed as per the guidelines and after approval of institutional animal ethics committee (IAEC no. 397/20) of National Institute of Immunology, New Delhi, India. Virus plaque-based neutralization assay was performed as per the guidelines of Infectious Disease Research Facility (biosafety level 3 facility) Translation Health Science and Technology Institute, New Delhi, India.

Consent for publication and authors role

All authors agreed to submit this manuscript. Manuscript conceptualization, data curation, formal analysis, investigation was done by AKP and JM. Writing original draft, review and editing was done by AKP, JM and PKS. JM, PKS, Sudeepa, JD, JV, MS, RA, NP, TQW, RK, GS, AG, SS were involved in methodology, project administration and resources.

Availability of data and materials

The datasets used and/or analyzed in the current study are available on reasonable request.

Declaration of Competing Interest

The authors declare that they have no known competing financial interests or personal relationships that could have appeared to influence the work reported in this paper.

References

[1] C.L. Atzrodt, I. Maknojia, R.D.P. McCarthy, T.M. Oldfield, J. Po, K.T.L. Ta, H. E. Stepp, T.P. Clements, A Guide to COVID-19: a global pandemic caused by the novel coronavirus SARS-CoV-2, FEBS J. 287 (17) (2020) 3633–3650.

[2] M.Y. Wang, R. Zhao, L.J. Gao, X.F. Gao, D.P. Wang, J.M. Cao, SARS-CoV-2: Structure, Biology, and Structure-Based Therapeutics Development, Front. Cell. Infect. Microbiol. 10 (2020) 587269.

[3] W. Tai, L. He, X. Zhang, J. Pu, D. Voronin, S. Jiang, Y. Zhou, L. Du, Characterization of the receptor-binding domain (RBD) of 2019 novel coronavirus: implication for development of RBD protein as a viral attachment inhibitor and vaccine, Cell. Mol. Immunol. 17 (6) (2020) 613–620.

[4] L. Premkumar, B. Segovia-Chumbez, R. Jadi, D.R. Martinez, R. Raut, A. J. Markmann, C. Cornaby, L. Bartelt, S. Weiss, Y. Park, C.E. Edwards, E. Weimer, E. M. Scherer, N. Rouphael, S. Edupuganti, D. Weiskopf, L.V. Tse, Y.J. Hou, D. Margolis, A. Sette, M.H. Collins, J. Schmitz, R.S. Baric, A.M. de Silva, The receptor binding domain of the viral spike protein is an immunodominant and highly specific target of antibodies in SARS-CoV-2 patients, Sci. Immunol. 5 (48) (2020).

[5] C.N. Fries, E.J. Curvino, J.L. Chen, S.R. Permar, G.G. Fouda, J.H. Collier, Advances in nanomaterial vaccine strategies to address infectious diseases impacting global health, Nat. Nanotechnol. 16 (4) (2021 Apr) 1–14.

[6] W. Wang, B. Huang, Y. Zhu, W. Tan, M. Zhu, Ferritin nanoparticle-based SARS-CoV-2 RBD vaccine induces a persistent antibody response and long-term memory in mice, Cell. Mol. Immunol. 18 (3) (2021 Mar) 749–751.

[7] E.J. Anderson, N.G. Rouphael, A.T. Widge, L.A. Jackson, P.C. Roberts, M. Makhene, J.D. Chappell, M.R. Denison, L.J. Stevens, A.J. Pruijssers, A.B. McDermott, B. Flach, B.C. Lin, N.A. Doria-Rose, S. O'Dell, S.D. Schmidt, K.S. Corbett, P.A. Swanson, M. Padilla, K.M. Neuzil, H. Bennett, B. Leav, M. Makowski, J. Albert, K. Cross, V. V. Edara, K. Floyd, M.S. Suthar, D.R. Martinez, R. Baric, W. Buchanan, C.J. Luke, V. K. Phadke, C.A. Rostad, J.E. Ledgerwood, B.S. Graham, J.H. Beigel, Safety and Immunogenicity of SARS-CoV-2 mRNA-1273 Vaccine in Older Adults, N. Engl. J. Med. 383 (25) (2020) 2427–2438.

[8] U. Sahin, A. Muik, E. Derhovanessian, I. Vogler, L.M. Kranz, M. Vormehr, A. Baum, K. Pascal, J. Quandt, D. Maurus, S. Brachtendorf, V. Lörks, J. Sikorski, R. Hilker, D. Becker, A.-K. Eller, J. Grützner, C. Boesler, C. Rosenbaum, M.-C. Kühnle, U. Luxemburger, A. Kemmer-Brück, D. Langer, M. Bexon, S. Bolte, K. Karikó, T. Palanche, B. Fischer, A. Schultz, P.-Y. Shi, C. Fontes-Garfias, J.L. Perez, K. A. Swanson, J. Loschko, I.L. Scully, M. Cutler, W. Kalina, C.A. Kyratsous, D. Cooper, P.R. Dormitzer, K.U. Jansen, Ö. Türeci, COVID-19 vaccine BNT162b1 elicits human antibody and TH1 T cell responses, Nature 586 (7830) (2020) 594–599.

[9] L.R. Baden, H.M. El Sahly, B. Essink, K. Kotloff, S. Frey, R. Novak, D. Diemert, S. A. Spector, N. Rouphael, C.B. Creech, J. McGettigan, S. Khetan, N. Segall, J. Solis, A. Brosz, C. Fierro, H. Schwartz, K. Neuzil, L. Corey, P. Gilbert, H. Janes, D. Follmann, M. Marovich, J. Mascola, L. Polakowski, J. Ledgerwood, B.S. Graham, H. Bennett, R. Pajon, C. Knightly, B. Leav, W. Deng, H. Zhou, S. Han, M. Ivarsson, J. Miller, T. Zaks, Efficacy and Safety of the mRNA-1273 SARS-CoV-2 Vaccine, N. Engl. J. Med. 384 (5) (2021) 403–416.

[10] Y.H. Chung, V. Beiss, S.N. Fiering, N.F. Steinmetz, COVID-19 Vaccine Frontrunners and Their Nanotechnology Design, ACS Nano 14 (10) (2020 Oct 27) 12522–12537.

[11] T.K. Tan, P. Rijal, R. Rahikainen, A.H. Keeble, L. Schimanski, S. Hussain, R. Harvey, J.W.P. Hayes, J.C. Edwards, R.K. McLean, V. Martini, M. Pedrera, N. Thakur, C. Conceicao, I. Dietrich, H. Shelton, A. Ludi, G. Wilsden, C. Browning, A.K. Zagrajek, D. Bialy, S. Bhat, P. Stevenson-Leggett, P. Hollinghurst, M. Tully, K. Moffat, C. Chiu, R. Waters, A. Gray, M. Azhar, V. Mioulet, J. Newman, A. S. Asfor, A. Burman, S. Crossley, J.A. Hammond, E. Tchilian, B. Charleston, D. Bailey, T.J. Tuthill, S.P. Graham, H.M.E. Duyvesteyn, T. Malinauskas, J. Huo, J. A. Tree, K.R. Buttigieg, R.J. Owens, M.W. Carroll, R.S. Daniels, J.W. McCauley, D. I. Stuart, K.-Y. Huang, M. Howarth, A.R. Townsend, A COVID-19 vaccine candidate using SpyCatcher multimerization of the SARS-CoV-2 spike protein receptor-binding domain induces potent neutralising antibody responses, Nat. Commun. 12 (1) (2021).

[12] L. Nunez-Munoz, G. Marcelino-Perez, B. Calderon-Perez, M. Perez-Saldivar, K. Acosta-Virgen, H. Gonzalez-Conchillos, et al., Recombinant Antigens Based on Non-Glycosylated Regions from RBD SARS-CoV-2 as Potential Vaccine Candidates against COVID-19, Vaccines (Basel) 9 (8) (2021).

[13] J. Meena, R. Kumar, M. Singh, A. Ahmed, A.K. Panda, Modulation of immune response and enhanced clearance of Salmonella typhi by delivery of Vi polysaccharide conjugate using PLA nanoparticles, Eur. J. Pharm. Biopharm. 152 (2020 Jul) 270–281.

[14] P.K. Smith, R.I. Krohn, G.T. Hermanson, A.K. Mallia, F.H. Gartner, M. D. Provenzano, E.K. Fujimoto, N.M. Goeke, B.J. Olson, D.C. Klenk, Measurement of protein using bicinchoninic acid, Anal. Biochem. 150 (1) (1985) 76–85.

[15] P. Singhvi, A. Saneja, S. Srichandan, A.K. Panda, Bacterial Inclusion Bodies: A Treasure Trove of Bioactive Proteins, Trends Biotechnol. 38 (5) (2020 May) 474–486.

[16] A. Vangala, D. Kirby, I. Rosenkrands, E.M. Agger, P. Andersen, Y. Perrie, A comparative study of cationic liposome and niosome-based adjuvant systems for

protein subunit vaccines: characterisation, environmental scanning electron microscopy and immunisation studies in mice, J. Pharm. Pharmacol. 58 (6) (2006 Jun) 787–799.

[17] P.H. Demana, N.M. Davies, S. Hook, T. Rades, Quil A-lipid powder formulations releasing ISCOMs and related colloidal structures upon hydration, J. Control. Release 103 (1) (2005 Mar 2) 45–59.

[18] P. He, Y. Zou, Z. Hu, Advances in aluminum hydroxide-based adjuvant research and its mechanism, Hum. Vaccin. Immunother. 11 (2) (2015) 477–488.

[19] L.A. Brito, M. Singh, Acceptable levels of endotoxin in vaccine formulations during preclinical research, J. Pharm. Sci. 100 (1) (2011 Jan) 34–37.

[20] M. Singh, H. Sori, R. Ahuja, J. Meena, D. Sehgal, A.K. Panda, Effect of N-terminal poly histidine-tag on immunogenicity of Streptococcus pneumoniae surface protein SP0845, Int. J. Biol. Macromol. 15 (163) (2020 Nov) 1240–1248.

[21] J. Meena, D.G. Goswami, C. Anish, A.K. Panda, Cellular uptake of polylactide particles induces size dependent cytoskeletal remodeling in antigen presenting cells, Biomater. Sci. 9 (23) (2021 Nov 23) 7962–7976.

[22] D.T. O'Hagan, E. De Gregorio, The path to a successful vaccine adjuvant–`the long and winding road`, Drug Discov. Today 14 (11–12) (2009 Jun) 541–551.

[23] V. Kanchan, Y.K. Katare, A.K. Panda, Memory antibody response from antigen loaded polymer particles and the effect of antigen release kinetics, Biomaterials 30 (27) (2009 Sep) 4763–4776.

[24] F. Sallusto, A. Lanzavecchia, K. Araki, R. Ahmed, From vaccines to memory and back, Immunity 33 (4) (2010 Oct 29) 451–463.

[25] A. Sokolovska, S.L. Hem, H. HogenEsch, Activation of dendritic cells and induction of CD4(+) T cell differentiation by aluminum-containing adjuvants, Vaccine 25 (23) (2007 Jun 6) 4575–4585.

[26] V.K. Singh, S. Mehrotra, S.S. Agarwal, The paradigm of Th1 and Th2 cytokines: its relevance to autoimmunity and allergy, Immunol. Res. 20 (2) (1999) 147–161.

[27] A. Getahun, J. Dahlstrom, S. Wernersson, B. Heyman, IgG2a-mediated enhancement of antibody and T cell responses and its relation to inhibitory and activating Fc gamma receptors, J. Immunol. 172 (9) (2004 May 1) 5269–5276.

[28] C.D. Rudulier, K.K. McKinstry, G.A. Al-Yassin, D.R. Kroeger, P.A. Bretscher, The number of responding CD4 T cells and the dose of antigen conjointly determine the TH1/TH2 phenotype by modulating B7/CD28 interactions, J. Immunol. 192 (11) (2014 Jun 1) 5140–5150.

[29] S. Tengvall, A. Lundqvist, R.J. Eisenberg, G.H. Cohen, A.M. Harandi, Mucosal administration of CpG oligodeoxynucleotide elicits strong CC and CXC chemokine responses in the vagina and serves as a potent Th1-tilting adjuvant for recombinant gD2 protein vaccination against genital herpes, J. Virol. 80 (11) (2006 Jun) 5283–5291.

[30] D.T. O'Hagan, R. Rappuoli, Novel approaches to vaccine delivery, Pharm. Res. 21 (9) (2004 Sep) 1519–1530.